18p

N63-14586

NASA TN D-1713

code-1

NASA TN D-1713

TECHNICAL NOTE

D-1713

A RADIATION VIEW OF HURRICANE ANNA FROM THE TIROS III METEOROLOGICAL SATELLITE

W. R. Bandeen, B. J. Conrath
W. Nordberg, and H. P. Thompson

Goddard Space Flight Center
Greenbelt, Maryland

NATIONAL AERONAUTICS AND SPACE ADMINISTRATION

WASHINGTON April 1963

554160

26p

A RADIATION VIEW OF HURRICANE ANNA FROM THE TIROS III METEOROLOGICAL SATELLITE

by
W. R. Bandeen, B. J. Conrath,
W. Nordberg, and H. P. Thompson
Goddard Space Flight Center

SUMMARY

The Tiros III meteorological satellite (1961 ρ1), containing two television cameras and a family of electromagnetic radiation experiments, was launched on July 12, 1961. Nine days later, the satellite passed directly over Hurricane Anna, the first hurricane of the 1961 Atlantic season. Data gathered by a five-channel medium resolution radiometer during one pass over the Hurricane are presented in the form of maps; and certain implications of the data are discussed. Supporting television pictures are also given.

The design and calibration of the medium resolution radiometer are briefly described.

CONTENTS

Summary i

INTRODUCTION. 1

DESIGN OF THE EXPERIMENT 1

CALIBRATION. 2

CONSTRUCTION OF THE MAPS 3

RESULTS 7

CONCLUSIONS. 14

ACKNOWLEDGMENTS 14

References 14

A RADIATION VIEW OF HURRICANE ANNA FROM THE TIROS III METEOROLOGICAL SATELLITE†

by
W. R. Bandeen, B. J. Conrath,
W. Nordberg, and H. P. Thompson
Goddard Space Flight Center

INTRODUCTION

The Tiros III meteorological satellite (1961 ρ1), launched on July 12, 1961, was the first of the Tiros series whose active lifetime extended over the peak of the Atlantic hurricane season. Two quasi-operational television camera systems carried by Tiros III observed every hurricane of the 1961 season. An experimental medium-resolution radiometer, scanning the earth and its atmosphere in five regions of the electromagnetic spectrum, also gathered data from the same storms from an orbital height of about 780 km.

The design of the radiometers, their calibration, the information flow, and the data reduction techniques have been discussed previously (References 1, 2, and 3). Also, the physical significance of the experiment and its potential synoptic use have been investigated (References 4 and 5).

In this paper, we shall discuss a sample of automatically processed radiation data gathered by Tiros III over the first tropical cyclone of the 1961 Atlantic season, Hurricane Anna.

DESIGN OF THE EXPERIMENT

To aid in understanding the radiation maps shown, the design and calibration of the radiation experiment should be discussed briefly here. The medium-resolution radiometer flown in Tiros III is practically identical to the first of its kind flown in Tiros II (1960 π1). There are five channels in the radiometer, each made sensitive to a different part of the electromagnetic spectrum by means of filters and other optical elements. The nominal bandwidths of the five channels are given in Table 1.

The radiometer employs a chopper which causes each sensor to view alternately, and at a rapid rate, in two directions 180 degrees apart. The response from each channel is proportional to the difference in the irradiation of the sensor bolometer from the two directions. The bidirectional axes of

†Presented at the International Symposium on Rocket and Satellite Meteorology, April 23-25, 1962, in Washington, D. C.

Table 1

Channel Bandwidths of the Tiros Five-Channel Medium Resolution Radiometer.

Channel	Nominal Bandwidth (microns)	Nature of Band
1	5.9-6.7	Water vapor absorption
2	7.5-13.5	Atmsopheric window
3	0.2-7.0	Reflected solar radiation
4	7.0-32.0	Terrestrial radiation
5	0.5-0.75	Response of the TV system

the channels are parallel to one another and inclined to the spin (camera) axis by 45 degrees. The satellite spins at about 9.3 rpm, causing the 5 degree instantaneous field of view to scan over the earth and space. The satellite's orbital motion advances the individual scan lines.

When viewing directly downward from a height of 780 km, the radiometer views a "spot" on earth with a diameter of about 68 km. As the nadir angle increases, the scan spot becomes increasingly elongated in the direction viewed. The satellite is spin stabilized, and as it revolves in orbit the radiometer scan geometry over the earth passes through a sequence of rather complicated patterns; however, in any configuration at least one direction of the sensors must always view outer space, which is essentially a zero reference for all five spectral regions. This zero reference is important in calibrating the instrument.

CALIBRATION

The preflight calibration of the three infrared channels is carried out by simulating the space-referenced earth signal in the laboratory. The radiometer's field of view is filled in one direction by a blackbody target at liquid nitrogen temperature (80°K) – which is essentially equivalent to the space reference—while the field of view in the other direction is filled with a blackbody target whose temperature is varied over the range expected when viewing the earth and its atmosphere. Thus, the measurements shown on the infrared maps are in terms of an "equivalent temperature, T_{BB}" of a blackbody filling the field of view which would cause the same response from the radiometer.

In calibrating the solar channels, one direction of the channels is merely masked with black tape to simulate space. To simulate reflected solar radiation from the earth and its atmosphere, a white diffuse reflector of known spectral reflectivity is illuminated at normal incidence from a standard lamp of known spectral intensity at a measured distance away, thus determining the spectral radiant emittance from the reflector. With the illuminated reflector filling the field of view, the output signal from each channel is measured. The spectral radiant emittance from the reflector is integrated over the spectral response curves of the solar channels to yield that portion of the radiation viewed to which each channel responds. The result of such integration is the "effective radiant emittance, $\overline{W}$." Thus, the measurements shown on the reflected solar radiation maps are in terms of that portion of diffuse radiation from a target filling the field of view to which each channel responds, $\overline{W}$. In order to interpret these measurements in terms of reflectance of insolation (or, loosely, "albedo"), we must know the effective radiant emittance, $\overline{W}^*$, which would be measured by each channel if the field of view were filled by a perfectly diffuse surface of unit reflectivity when illuminated by one solar constant at

normal incidence. The values of $\overline{W}^*$ for channels 3 and 5 have been calculated to be, respectively, 763.8 w/m^2 and 108.6 w/m^2.

Obviously, any uncertainties in the spectral response curves of the solar channels will cause uncertainties in the subsequent calculations of $\overline{W}$ and $\overline{W}^*$ values. Because of the broad spectral response of channel 3, uncertainties have a much larger effect on this channel than on channel 5. Therefore, we have less confidence in the *absolute* measurements of channel 3 than of channel 5, although the relative measurements for both channels are accurate to within about 3 percent.

CONSTRUCTION OF THE MAPS

The maps shown in Figures 1 through 5 were produced by automatic data processing techniques; the shading between contours was done manually to enhance the display. Figure 2b was specially produced at a scale twice as large as in the other maps and the isotherms were hand-traced and labeled to increase resolution in displaying the data.

In producing the maps (except Figure 2b), a computer program distributed all data having a sensor nadir angle of 58 degrees or less during the period from 1545 to 1602 GMT, July 21, 1961, over a

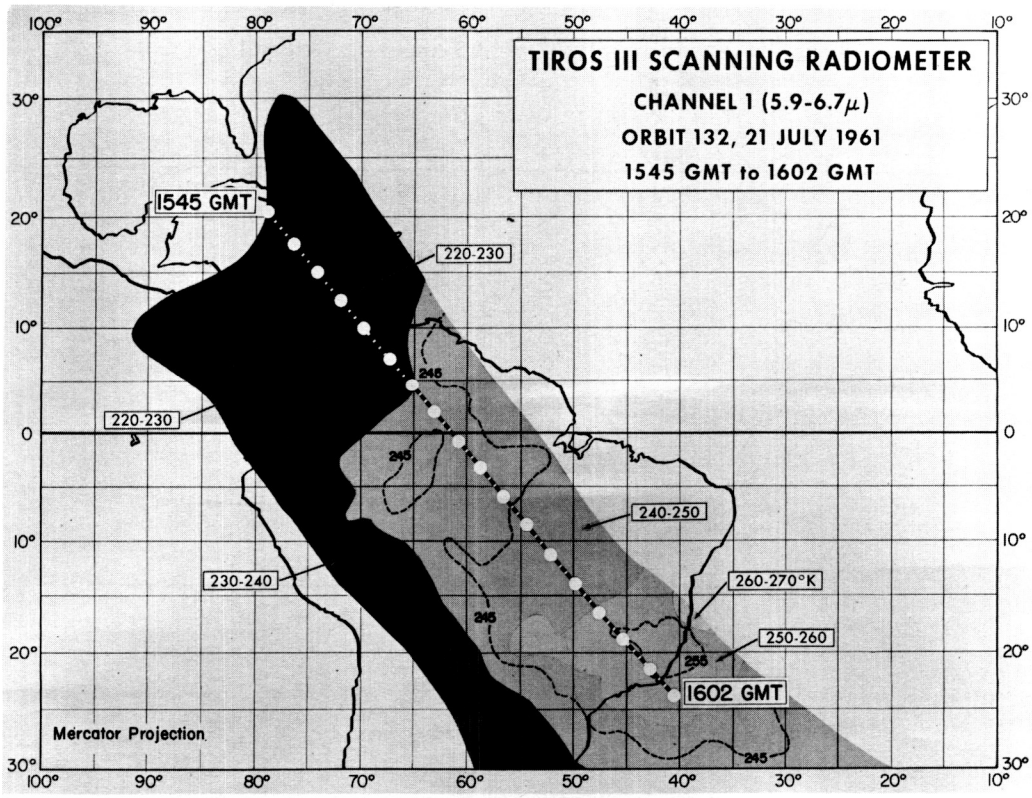

Figure 1—Radiation map from the Tiros III scanning radiometer: channel 1 (5.9 to 6.7 microns), orbit 132 1545-1602 GMT, July 21, 1961. Hurricane Anna is centered at latitude 13.8°N, longitude 72.3°W. Original grid scale: 2.5 degrees of earth longitude per mesh interval. The subsatellite track is shown with subsatellite points indicated by dots for each minute of time.

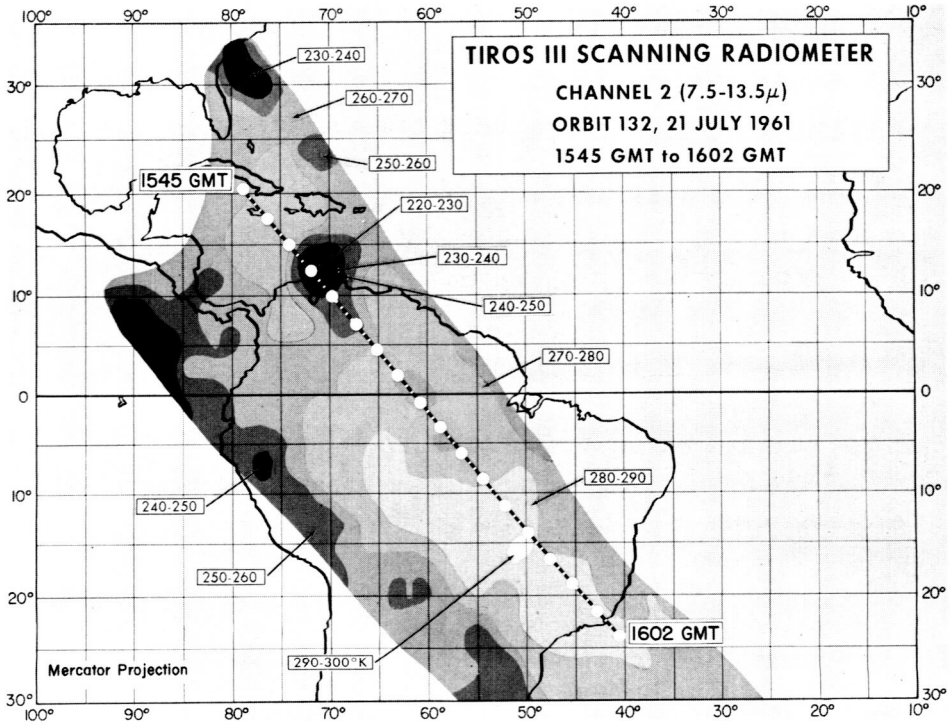

Figure 2a—Radiation map: channel 2 (7.5-13.5 microns). Original grid scale 2.5 degrees per mesh interval.

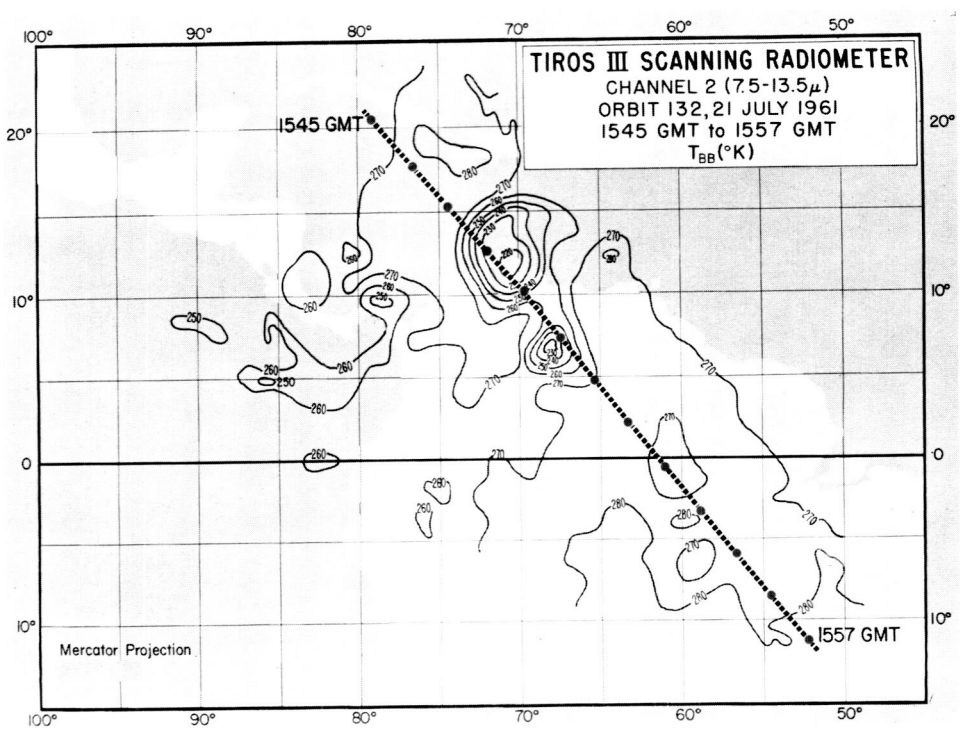

Figure 2b—Detailed map of a section of Figure 2a. Original grid scale 1.25 degrees per mesh interval.

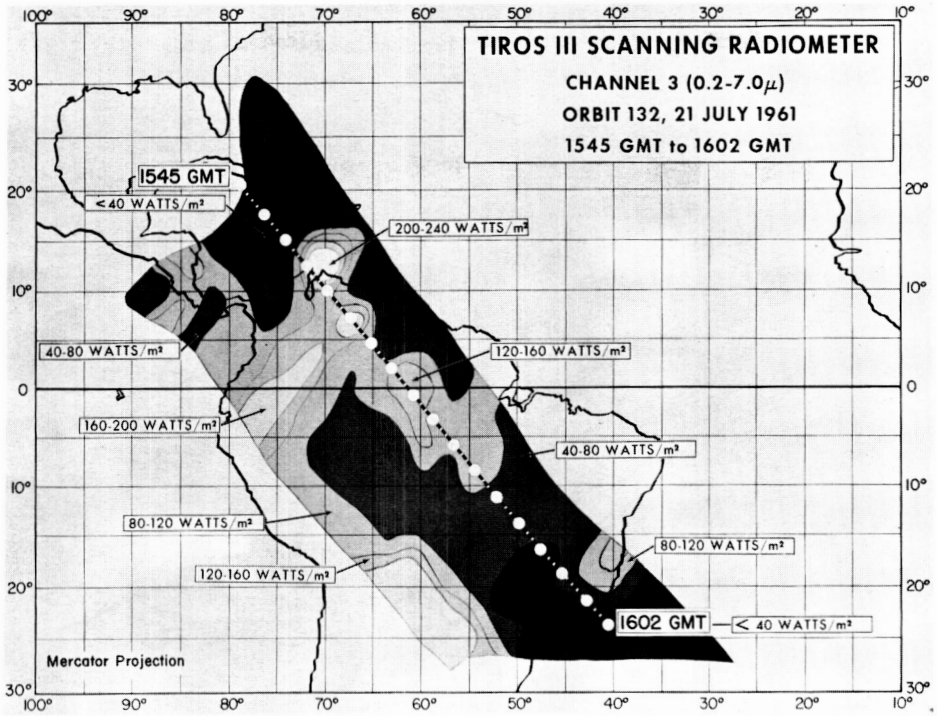

Figure 3—Radiation map: channel 3 (0.2-7.0 microns). Original grid scale 2.5 degrees per mesh interval.

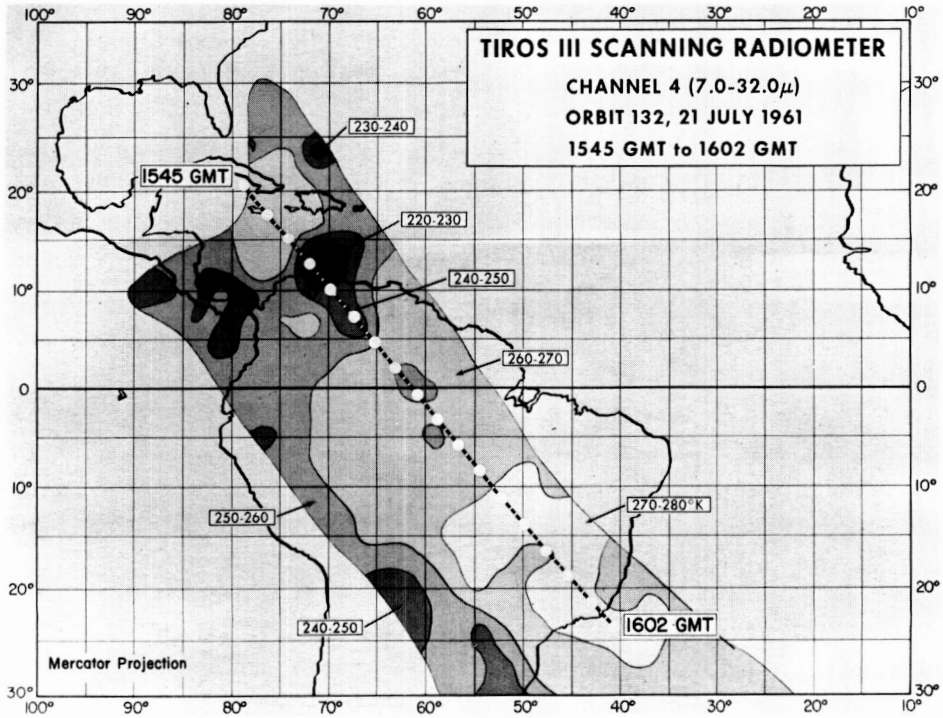

Figure 4—Radiation map: channel 4 (7.0-32.0 microns). Original grid scale 2.5 degrees per mesh interval.

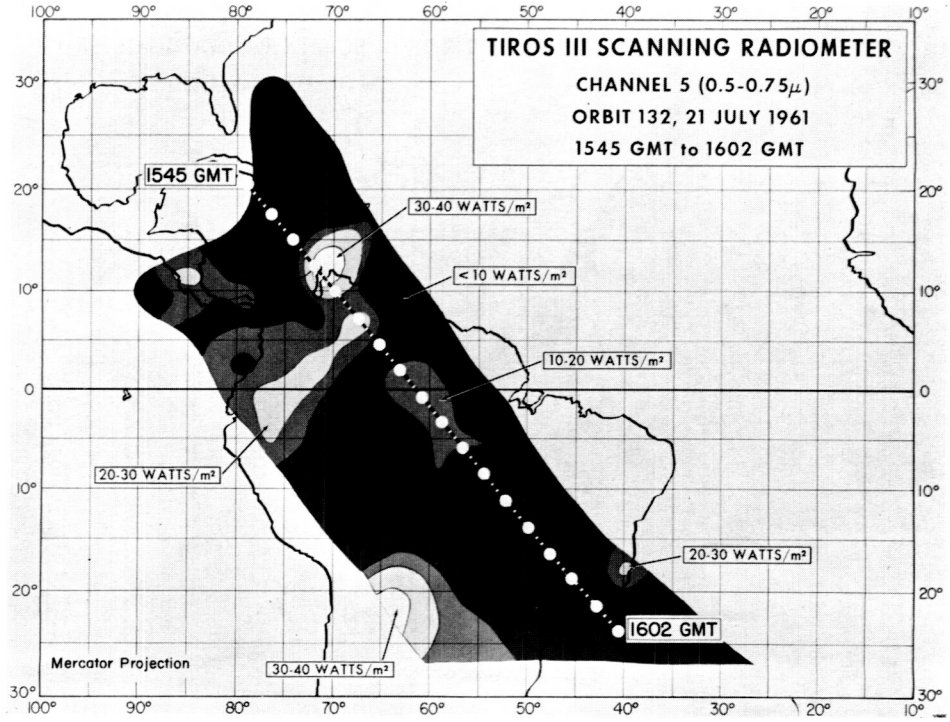

Figure 5—Radiation map: channel 5 (0.5-0.75 microns). Original grid scale 2.5 degrees per mesh interval.

grid field with a mesh interval between points of 2.5 degrees of longitude (about 278 km square at the equator). Figure 2b was produced in the same way, except that data from 1545 to 1557 GMT were used and the mesh interval between grid points was 1.25 degrees of longitude, thus increasing the resolution by about a factor of four. The population of measurements within a mesh interval varied from 1 along the southwestern edge to more than 60 (or about one-fourth of this number for Figure 2b) along the northeastern edge of the data area. This large variance results from the complicated nature of the scan. The minimum spin axis (TV camera axis) nadir angle was 16.0 degrees and occurred at 1558:30 GMT. The subsatellite track is shown on all maps, with subsatellite points indicated by dots for each minute of time. The displacement of the data "center of mass" with respect to the subsatellite track is evidence that the camera principal point track lay southwest of the subsatellite track. The computer averages the individual measurements within each mesh interval, accomplishes the contouring of the grid point averages with filler numbers, and prints the maps on a high speed printer. A Mercator latitude-longitude overlay completes the grid print map and locates the data geographically. The maps shown in Figures 1 through 5 have been produced by replacing the filler numbers by shading between contour intervals (or tracing the isotherms in Figure 2b).

Two limitations of this form of data display are re-emphasized: (1) the direction from which a measurement is made (i.e., nadir or zenith and azimuth angles) is not readily apparent, and (2) the number of individual measurements making up each grid point average (or the amount of data smoothing) is not readily apparent. These limitations must be kept in mind when attempting to interpret such maps.

RESULTS

Hurricane Anna moved from a point just north of Venezuela to the coast of British Honduras during the period July 20-24, 1961. At 1550 GMT on July 21, Anna was centered at latitude 13.8°N, longitude 72.3°W, and still growing in intensity. Orbit 132 of Tiros III passed almost directly over the hurricane at that time, and the satellite's attitude was such that all radiometer measurements over Anna were made under sensor nadir angles of less than 15 degrees. Figures 1 through 5 show the stark relief in which the hurricane stands out from its surroundings in all five spectral regions. Three television pictures (Figures 6, 7, and 8) taken by Tiros III at about this time show Anna, the extensive cloudiness just to the south of it, and the scattered-to-clear regions over equatorial South America.

Figure 6—Television picture taken by Tiros III on orbit 132, July 21, 1961 at 1549:50 GMT. Hurricane Anna is the upper cloud mass, centered about 70 miles north of the Guajira Peninsula of Colombia. The Colombian coast runs horizontally to the west and joins Panama (near the upper left fiducial mark). Lake Maracaibo is cradled in the upper right-hand quadrant of the central fiducial cross.

Figure 6 shows Anna centered about 70 miles north of the Guajira Peninsula, with the Colombian coastline running laterally to the west and joining Panama. Lake Maracaibo is cradled in the upper right-hand quadrant of the central fiducial cross. A second extensive cloud system is seen south of Anna over Venezuela. The temperatures shown in Figures 2 and 4 clearly outline this second system and indicate that its mean top is at a lesser height than that of the hurricane. Also, the increased temperatures on these maps over the region stretching from Venezuela to Peru indicate that the band of clouds shown here on the solar maps is at a still lower height, or is thinner, or both.

The hurricane stands out clearly in channels 3 and 5. The actual maximum $\overline{W}$ measurement over Anna from channel 3 was $240\,w/m^2$ and from channel 5 was $40\,w/m^2$. The subsolar point at 1550 GMT was at latitude 20.4°N, longitude 55.9°W, some 18 degrees from the storm center. Taking the solar radiation incident upon the hurricane as $\overline{W} \cdot \cos 18°$, the maximum reflectance r of sunlight in the direction of the satellite is

$$\text{for channel 3:} \quad r = \frac{240}{763.8 \cos 18°} = 33.0 \text{ percent;}$$

$$\text{for channel 5:} \quad r = \frac{40}{108.6 \cos 18°} = 38.7 \text{ percent;}$$

The maximum r measured by channel 3 is 5.7 percent lower than at measured by channel 5. As was mentioned earlier, measurements by channel 3 might be somewhat in error because of the lack of an accurate measurement of its spectral response. This fact might very well be responsible for the observed difference in r. Of course, this discrepancy does not affect the validity of the relative radiation levels and, therefore, the ability of the data to map cloud systems.

The patterns in the maps of the solar channels are very similar. The large cloud system south of the hurricane over Venezuela and the band of cloudiness stretching from it southwest across Colombia into Northern Peru stand out clearly in Figures 3 and 5, and can be identified in the television pictures in Figures 7 and 8. The high reflectance region around latitude 22°S and longitude 63°W implies the presence of clouds, but the relatively high temperatures measured by channel 2 indicate that the cloud tops were not very high. The broad band of high channel 2 temperatures running from the Amazon basin across Brazil to the Atlantic Ocean compares well with the low solar channel measurements, implying that there are few clouds and that the effective height of radiation of the window channel is near the surface. The channel 4 and channel 1 maps also show a similar pattern, and the photograph in Figure 8 reveals the scattered-to-clear condition over the Amazon region of Brazil.

The region north of latitude 30°N off Florida is mapped only by channel 2, where values of T_{BB} below 240°K are shown. Widespread cumulonimbus clouds with anvil tops were reported in this region at the time, and undoubtedly contributed to the low temperatures observed. However, a complication in interpreting measurements in this region is that they were all made at nadir angles of nearly 58 degrees. The comparable zenith angles at the top of the atmosphere were about 72 degrees, meaning that the radiometer was viewing through more than three atmospheres. Under these conditions, limb darkening effects become appreciable, even in the window channel, and caution must be used in interpreting the data.

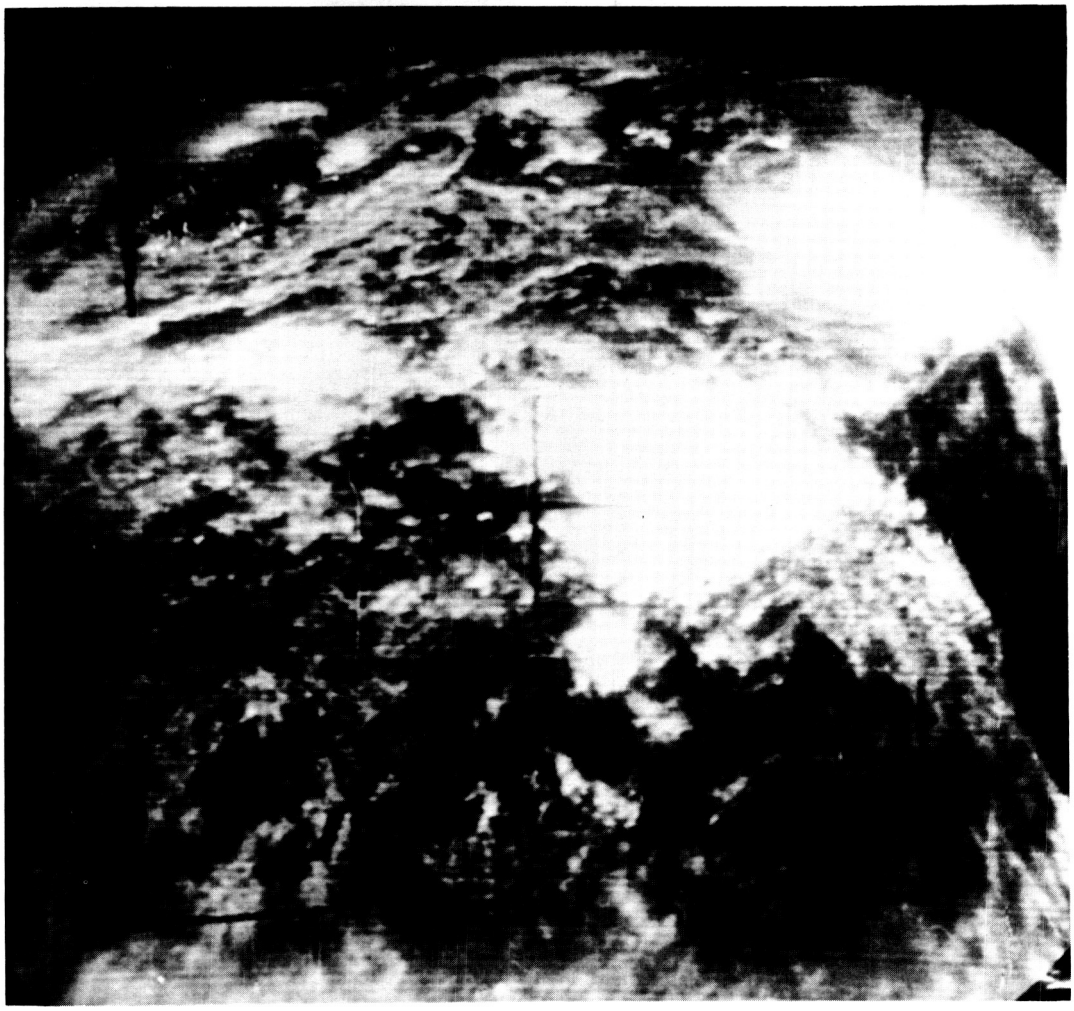

Figure 7—Television picture taken by Tiros III, orbit 132, July 21, 1961 at 1550:50 GMT. The central cloud mass is over Venezuela with Hurricane Anna to the north. The Colombia coast running westward to Panama is seen at the top of the picture.

Actually, each infrared channel "sees" many different layers in the atmosphere. The contribution of each atmospheric layer to the integrated response of a particular channel depends upon the vertical distributions of temperature, pressure, and the various infrared absorbers (primarily H_2O, CO_2 and O_3); and upon the positions and strengths of the various absorption bands with respect to the spectral response curve of the particular channel. Because of strong absorption by water vapor in the 6.3 micron band, generally (in the absence of clouds) a broad region throughout the middle and upper troposphere predominates in contributing to the response of channel 1, with little or no contribution from the surface of the earth.

Because of only weak absorption by ozone and water vapor in the atmospheric window, radiation from the surface of the earth or from clouds predominates in the response of channel 2, with small contributions from the atmosphere. Because channel 4 includes the window as well as strong water vapor and carbon dioxide absorption bands, it receives important contributions from both earth and

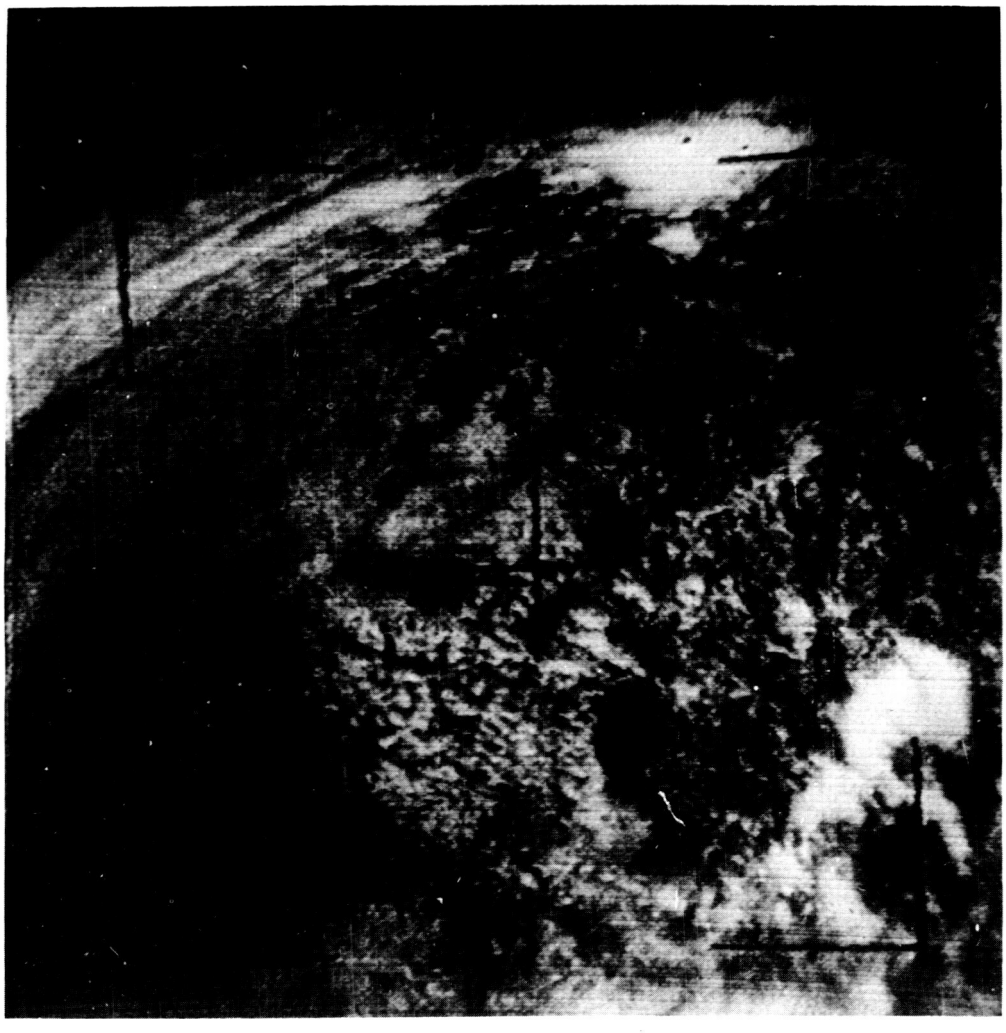

Figure 8—Television picture taken by Tiros III, orbit 132, July 21, 1961 at 1552:20 GMT. The cloud mass which is south of Hurricane Anna is seen at the top of the picture. The central fiducial cross is near the headwaters of the Orinoco River in southern Venezuela. The lower portion of the photograph reveals the scattered-to-clear condition over the Amazon region of Brazil.

atmosphere. The air temperature generally decreases with height in the troposphere where a preponderance of the important absorbers is found; hence, it follows that usually the equivalent blackbody temperatures T_{BB} measured by channel 1 should be lowest, those measured by channel 2 highest, and those measured by channel 4 somewhere between the first two. This pattern generally prevails throughout Figures 1, 2, and 4, with T_{BB} highest in channel 2, 20 degrees lower in channel 4, and 20 to 40 degrees lower in channel 1. The one exception to this pattern is over the hurricane, where the T_{BB} values for all channels are indicated as 220 to 230°K.

If we define a fictitious level, called the "effective height of radiation," as the height at which the T_{BB} measured by the satellite corresponds to the real atmospheric temperature, it follows from the previous paragraph that the effective height of radiation for channel 1 should be highest and that for channel 2 lowest, with the channel 4 height falling in between. Fritz and Winston (Reference 5) have

shown that the effective height of radiation from the window channel of Tiros II affords a good estimate of the heights of the tops of large-scale overcast clouds, although cirrus are not clearly defined because they are partially transparent.

From radiosonde data taken near the hurricane, the ambient air temperature ranged from 230 to 220°K in the height interval from about 11,000 to 12,100 meters implying that the smoothed mean height of the hurricane clouds as mapped in Figure 2 lay within this layer. However, the smoothing contained in the grid point averages and the 10°K contour intervals used in the maps obscure much of the fine structure which is possible within the 5 degree field of view.

For example, a computer listing of the individual data points making up the maps revealed three individual spots (a spot diameter on earth is about 68 km) over the hurricane where there was a dramatic reversal of the usual order of T_{BB} measurements from the infrared channels coincident with the minimum observed channel 2 temperatures. These three spots, each from a different swath, yielded the values of T_{BB} shown in Table 2. The temperature and height of the tropopause averaged from 1200 GMT radiosonde runs made at Kingston, Jamaica, Trinidad, and Swan Island were about 199.5°K and 16,000 meters, respectively. The estimated absolute accuracy of channel 2 is ±5°K. Therefore, the minimum T_{BB} for channel 2 was probably between 199.5° and 206°K (i.e., 201° + 5°K), and its effective radiating height was probably within 1500 meters of the tropopause. It can therefore be inferred that the highest overcast clouds were within about 2000 meters of the tropopause. The reversal of the usual pattern of T_{BB} measurements can be explained qualitatively by considering an upward translation of the usual effective radiation height sequence (i.e., that for channel 1 highest and that for channel 2 lowest) such that the effective radiation height for the window channel is at or near the tropopause, with the others located above the inversion where temperature increases with height.

The estimated absolute accuracy of channel 1 is ±5°K. Therefore, the observed channel 1 T_{BB} corresponding to the minimum observed channel 2 T_{BB} might have been as low as 228° − 5° = 223°K. It seems difficult to justify sufficient water vapor in the stratosphere to account for a difference in channel 1 and channel 2 T_{BB} measurements of even 17°K (i.e., 223° - 206°). However, the following preliminary calculations, assuming plausible temperature and water vapor profiles for the tropical stratosphere (Figure 9), do indicate that differences of at least 10.5°K may indeed be possible, indicating the state of the atmosphere above tropical storms. Reasonable variations about the temperature and water vapor profiles chosen and in the theoretical assumptions regarding absorption could probably yield differences of as much as 17°K.

The specific intensity emerging from the "top" of the atmosphere I is given by the solution of the radiative transfer equation, which may be written in the form

$$I = I_0 \tau_0 + \int_{\tau_0}^{1} B[T(u)]\, d\tau(u)$$

Table 2

Reversal of the Usual Order of Infrared Channel Temperatures in Three Spots Over Hurricane Anna.

Channel	Nominal Bandwidth (microns)	T_{BB} (°K)		
		Spot 1	Spot 2	Spot 3
1	5.9-6.7	225	228	228
4	7.0-32.0	219	212	215
2	7.5-13.5	205	207	201

where I_0 is the specific intensity at the bounding surface (ground or cloud as the case may be), B is the Planck function, and τ is atmospheric transmission above a level at which the optical depth is u. If τ and the temperature are known as functions of u, then this calculation can be carried out.

In practice, the integral can be evaluated by means of radiation diagrams. A diagram of the Möller type was employed in this particular work. This diagram was for a spectral interval of from approximately 6.33 to 6.85 microns, while the channel 1 spectral range of the radiometer was about 6.0 to 6.6 microns. However, the calculations based on the 6.33 to 6.85 micron range should serve to indicate whether the differences observed between channels 1 and 2 are of the right order or not.

Calculations were carried out for cloud tops at and slightly below the tropopause height. The results are shown in Figure 10 in which the cloud top temperature as seen by the window channel is plotted against the difference between the temperature seen in the window and that seen in the water vapor absorption region.

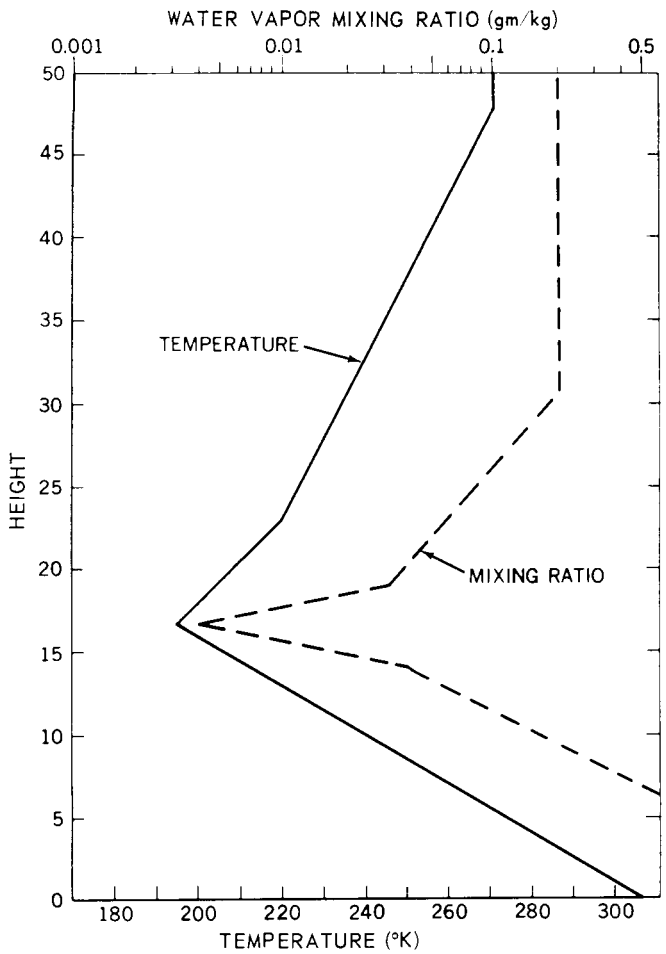

Figure 9—Temperature and water vapor mixing ratio profiles assumed in the theoretical calculations attempting to explain the "reversed" relative behavior of channels 1 and 2 over tropical storm systems.

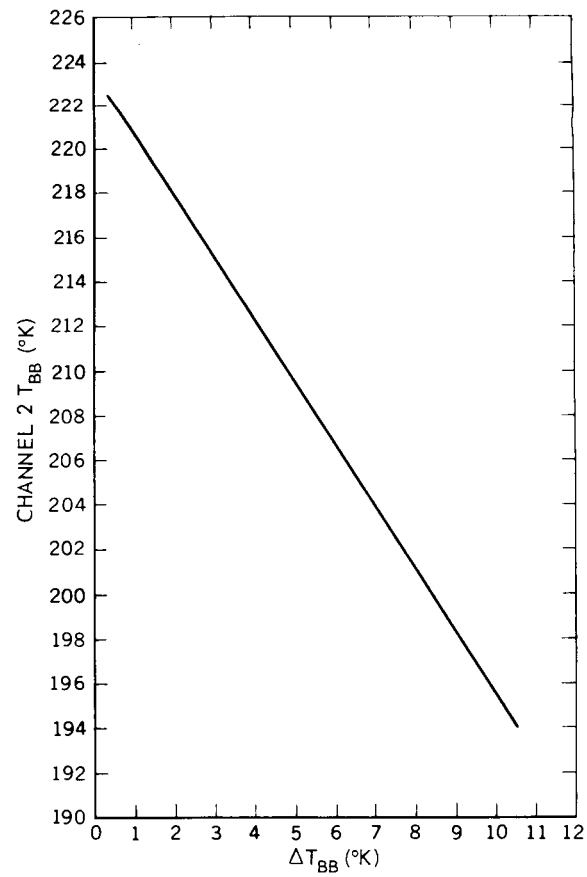

Figure 10—Results of the theoretical calculations. Cloud top temperature, which is assumed to be that seen by channel 2, is shown as the ordinate (channel 2 T_{BB}). The abcissa, ΔT_{BB}, is the difference between the effective blackbody temperature seen in the window region and that seen in the water vapor absorption region.

Only one other case of a channel 1 - channel 2 temperature reversal has been noted in all of the Tiros III radiation data analyzed to date, although it has not been possible yet to survey comprehensively all data and rule out still other occurrences of this phenomenon. This case was associated with a storm system shown in Figure 11 which is a picture taken over northwest Africa on July 17, 1961. The African coast line and the Atlantic Ocean can be seen in the upper left corner.

Table 3

Reversed Data Points in Two Spots Over a Cloud System Shown in Figure 11.

Channel	Nominal Bandwidth (microns)	T_{BB} (°K)	
		Spot 1	Spot 2
1	5.9-6.7	213	211
2	7.5-13.5	201	205

Figure 11—Photograph taken over northwest Africa by Tiros III at about 1309 GMT on July 17, 1961. The African coast line and the Atlantic Ocean can be seen in the upper left corner.

When the cloud system just above the central fiducial cross in the photograph was scanned by the radiometer, the "reversed" data points shown in Table 3 taken from two different swaths were found. While the temperature differences seen in these data points are smaller than those associated with the hurricane, they are still probably real and serve to further substantiate the phenomenon of reversed relative behavior of channels 1 and 2. Obviously, much more work is required in this area, and we hope to be able to report additional information at a later time.

CONCLUSIONS

The radiation maps of Hurricane Anna show that a severe storm of this type stands out clearly in all three infrared channels, and, in the daytime, also in the two solar channels of the Tiros medium resolution radiometer. The synoptic use potential of such radiation data in future meteorological satellites seems clear for complementing and augmenting television cameras in the identification and tracking of severe weather systems.

The extraordinary reversal of the usual order of equivalent blackbody temperatures over the hurricane, together with the low channel 2 measurement, suggest that the cloud tops over Hurricane Anna were very high—probably near the height of the tropopause. The magnitude of the difference between the equivalent blackbody temperatures measured by channel 1 and channel 2 infer a very wet stratosphere with a sharp temperature inversion above the cloud tops. However, much more work in this area remains to be done before definite conclusions can be drawn.

ACKNOWLEDGMENTS

The authors wish to express their thanks to Mr. Robert Hite, of Goddard Space Flight Center, who wrote the primary radiation data reduction program, and to Mr. William Callicott, United States Weather Bureau, who wrote the mercator mapping program used in the automatic computer processing of the radiation data given in this paper.

REFERENCES

1. Bandeen, W. R., Hanel, R. A., Licht, J., Stampfl, R. A., and Stroud, W. G., "Infrared and Reflected Solar Radiation Measurements from the Tiros II Meteorological Satellite," *J. Geophys. Res.* 66(10): 3169-3185, October 1961.

2. Nordberg, W., Bandeen, W. R., Conrath, B. J., Kunde, V., and Persano, I., "Preliminary Results of Radiation Measurements from the Tiros III Meteorological Satellite," *J. Atmosph. Sciences* 19(1): 20-30, January 1962.

3. Hanel, R. A., and Stroud, W. G., "The Tiros II Radiation Experiment," *Tellus* 13(4):486-488, November 1961.

4. Hanel, R. A., and Wark, D. Q., "Tiros II Radiation Experiment and its Physical Significance," *J. Opt. Soc. Amer.* 51(12):1394-1399, December 1961.

5. Fritz, S., and Winston, J. S., "Synoptic Use of Radiation Measurements from Satellite Tiros II," *Monthly Weather Review* 90(1):1-9, January 1962.

6. Gutnick, M., "How Dry is the Sky?" *J. Geophys. Res.* 66(9):2867-2871, September 1961.

7. Nordberg, W., and Stroud, W. G., "Seasonal, Latitudinal, and Diurnal Variations in the Upper Atmosphere," NASA Technical Note D-703, April 1961.